Using Pulsed Lasers as a Diagnostic Tool for Radiation-Induced Single-Event Latchup

Andrew Sternberg
Institute for Space and Defense Electronics, Vanderbilt University
1025 16th Ave S, Nashville, TN 37212
Andrew.l.sternberg@vanderbilt.edu

Robert A. Reed, Ron D. Schrimpf, Peng Wang
Department of Electrical Engineering and Computer Science, Vanderbilt University
Robert.a.reed@vanderbilt.edu
Ron.schrimpf@vanderbilt.edu
Peng.wang@vanderbilt.edu

John Kozub
Department of Physics and Astronomy, Vanderbilt University
John.kozub@vanderbilt.edu

ABSTRACT

Femtosecond pulsed lasers are a useful diagnostic and screening tool when evaluating electronic parts for potentially destructive radiation-induced single-event effects such as single-event latchup (SEL). Pulsed lasers may be used to estimate sensitive cross-sections and for comparing the relative sensitivity of equivalent parts.

INTRODUCTION

The natural radiation environment of space is well known to have deleterious effects on electronic components. Total-ionizing dose received primarily from high-energy protons and electrons and bremsstrahlung x-rays may cause a gradual degradation of device performance, leading to eventual failures. Energetic ions emanating from the sun or from galactic sources may cause more immediate effects, known as single-event effects (SEE). These may appear as transients in analog or digital circuits. Heavy-ions may also cause bit-flips in sequential logic and memory cells, leading to effects such as data corruption or incorrect state machines.

Another class of potentially destructive events exists. This class includes burnout and breakdown in power devices and single-event latchup (SEL).

While the transient and bit-flip events may cause corruption or interrupt functionality, they are potentially recoverable using techniques such as scrubbing, reprogramming, or simply rebooting. In contrast, SEL, as the name implies, is a latchup event which may lead to sustained high-current that can cause localized heating, possibly damaging junctions, melting metallization, or burning out bond wires.

Techniques exist for detecting and mitigating SEL, however, latent damage may shorten the lifetime of the part or impair performance. Mitigation techniques may also add complexity to the system, making failure analysis more difficult. It is important to understand the frequency and nature of these latchup events to best design mitigation techniques.

The traditional method for measuring SEL involves exposing the part under normal or worst-case operating conditions to heavy-ion or proton beams at an accelerator facility. These facilities may be very expensive, but permit the user to measure the number of latchup events for ions of different linear-energy transfer (LET) at a specified flux. This information can be convolved with the spectrum of heavy ions present at a particular orbit and solar environment to estimate the rate at which SEL will occur. If the SEL rate is below the acceptable risk for the mission then no changes are needed.

If corrective actions are required, one may choose to use SEL detection circuitry, or replace the part with one having better SEL performance. Radiation-hardened parts, when they exist, are often outside of the budget for many small-satellite programs. This leaves satellite designers searching for commercial replacement parts which may have lower SEL cross-sections, higher SEL thresholds, or even be SEL immune.

There are several databases (JPL[1], NASA GSFC[2], ESA[3]) which maintain radiation performance data on a variety of parts. In addition, radiation test results may also be found in publications such as IEEE Transactions on Nuclear Science (TNS), IEEE Radiation Effects Data Workshop, and Radiation and its Effects on Components and Systems (RADECS) proceedings. Unfortunately, these databases only cover a small fraction of all the electronic components available today.

SEL can be very sensitive to the device fabrication process. Given that many vendors operate multiple fabrication facilities, or outsource part or even all of their fabrication to third parties, it is frequently the case that older radiation data are no longer applicable to recently purchased parts. For low-volume customers, it may be nearly impossible to purchase all their parts from a known lot or wafer run. Thus, if designers want to know the SEL sensitivity of a particular part, they must have either some knowledge of the fabrication process or test data.

At Vanderbilt University, we have been developing pulsed laser systems for investigating various transient effects on devices and circuits [4-7]. The pulsed laser has been very useful for both fundamental science studies on novel devices and materials and in applied circuit scenarios. In this paper will demonstrate the pulsed-laser's applicability to SEL testing through the use of dedicated test structures known to have a certain latchup behavior based on previous heavy-ion testing.

SINGLE-EVENT LATCHUP (SEL)

SEL is a sustained high-current phenomenon resulting from parasitic thyristor structures which are part of the normal CMOS fabrication process. SEL may be understood as a positive feedback process from the complementary NPN and PNP transistors formed by device wells and junctions, as shown in Figure 1. A NPN transistor is formed between the source of the NMOS transistor (emitter), p-substrate (base) and n-well (collector). A PNP transistor is formed by the source of the PMOS transistor (emitter), n-well (base) and p-substrate (collector). Parasitic resistances are also present; the most important ones are indicated. A schematic representation of this arrangement of parasitic devices is shown in Figure 2. All of these junctions are reverse-biased under normal operating conditions. However, charge introduced into the circuit from a heavy ion can cause a junction to become forward biased. If the NPN transistor in Figure 2 begins to conduct, a voltage will be dropped across the n-well resistance. If this voltage exceeds the turn-on voltage for the PNP transistor, it will begin to conduct. This will cause current to flow in the substrate resistance, turning the NPN transistor on more. This positive feedback loop may cause a damaging amount of current to flow through these devices.

Several conditions must exist for SEL to occur. The first is that the product of the transistor beta values must be > 1 for a regenerative path to be maintained. The second is that the supply voltage must be greater than 2xVBEon, which is usually around 1.2V. Thus, circuits operating at 0.9V are usually not susceptible to SEL. However, many such circuits, while having a core running at 0.9V will have interface and I/O circuits operating at 1.2-3.3V and will be susceptible to SEL.

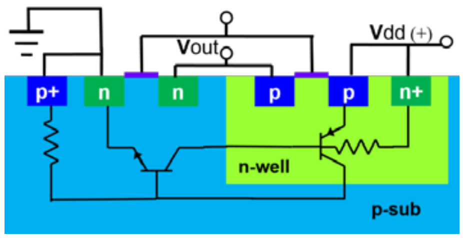

Figure 1 - Diagram showing parasitic transistor structures in a typical CMOS process

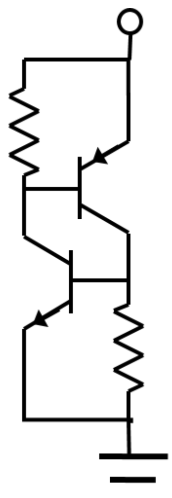

Figure 2 - Schematic representation of parasitic NPN and PNP structures forming a regenerative feedback path.

Devices built on SOI or SOS wafers are typically not SEL sensitive. However, not all SOI devices are fully dielectrically isolated, so parasitic transistors may still be present.

LASER SEE SIMULATION

Lasers have been used since the 1960's to simulate SEE in semiconductor devices [8]. Lasers with photon energies above the bandgap of the semiconductor can directly generate electron-hole pairs through ionization. The liberated charge is swept across junctions by the electric field or diffuses to junctions where it may be collected. This is similar to what happens during a heavy-ion strike, although the charge-generation mechanism is different.

Because the photons have a high probability of being absorbed, the intensity drops off quickly inside the semiconducting material. The 1/e depth for 532 nm photons in intrinsic silicon is approximately 1.3 µm. Much of the energy is absorbed at the surface with less being absorbed in the substrate. In contrast, 1260 nm photons have a 1/e depth of about 27 m.

Metallization poses another problem for laser testing. Analog integrated circuits (ICs) with two or three metal layers and large devices may be tested with a laser. For modern submicron CMOS process with many metal layers, there is no way to penetrate through the metal layers to reach the semiconducting material.

To work around these limitations, we are using a non-linear optical technique known as two-photon absorption (TPA [9]). TPA uses photons with energies less than the bandgap of the semiconductor. This means they are not absorbed – the semiconductor is transparent to these photons. However, if we focus the beam to a very small spot, the intensity near the focal point is great enough that multiple photons may interact to generate electron-hole pairs. Since this occurs only where the intensity is highest, we are able to translate the beam deeper in the device to stimulate junctions at different depths.

This property allows us to shoot the laser into the backside of the IC, avoiding the problem of metallization. Care is needed in preparing the samples and will be discussed in a subsequent section.

PULSED LASER SYSTEM

The TPA laser technique requires very short laser pulses for two primary reasons. The first is to generate the intensities required for TPA. A typical pulse energy is on the order of a nanojoule. The intensity at the focus of a beam can reach on the order of 100's of GW/cm^2.

The second reason to have very short pulses is to have the charge generation take place much faster than the device can respond.

Pulse Generation

Figure 3 is a photograph of the laser system in use at Vanderbilt University. A diode-pumped continuous wave (CW) laser feeds a passively mode-locked oscillator. The mode-locked output is a train of pulses about 150 fs wide at a repetition rate of about 80 MHz. This output "seeds" a laser-pumped TiS amplifier. The amplifier is Q-switched, producing a high-intensity pulse at a repetition rate of 1 kHz. The output of the amplifier feeds an optical parametric generator (OPG). The OPG uses nonlinear crystals to mix the input beams with multiples of their respective wavelengths to produce ultrafast pulses at wavelengths from ultraviolet to infrared. This wide range of wavelengths enables us to generate photons useful for single and two-photon absorption processes in materials other than silicon.

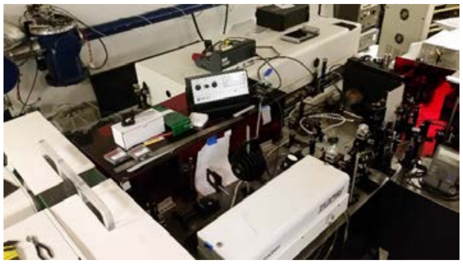

Figure 3 – Photograph of the ultrafast laser at Vanderbilt.

Test Station

Multiple photon energies leave the OPG. A prism separates the wavelengths and sends the correct wavelength and to the turning mirrors. A 1-to-1 telescope with a pinhole located near the focus is used to clean up the beam and remove any structure at the beam edges. The beam then passes through a shutter and a linearly graded neutral density filter wheel which goes from OD0 to OD2. The filter wheel is attached to a motor which causes it to act as an energy modulator. A set of crossed wire-grid polarizers allows manual intensity tuning and is used to set the maximum intensity of the laser pulse.

From there, the laser enters the black box. The black box contains two beam splitters. The first beam splitter reflects a portion of the beam to a calibrated photodiode for energy measurement. It is important that we measure the energy for every pulse since the laser energy may vary slightly from one pulse to the next. The second beam splitter reflects a portion of the return image on to a CCD camera that is used to view the backside of the device.

As the beam leaves the black box, it is turned up through a 100X NIR Plan Apo microscope objective. Additionally, light from a fiber-coupled broadband source is also directed into the objective for surface illumination. The microscope objective focuses the beam to a spot whose diameter approaches the diffraction limit. For most experiments, this is around 1.5 micrometers. The microscope objective is mounted on a z-axis linear translation stage that moves relative to the turn-up mirror. We use this to compensate for changes in DUT mounting, package height, and die thickness. We can also use this z-axis motion to generate charge at different depths in the substrate.

The broadband illumination contains a significant portion in the near infrared and is thus able to penetrate through the silicon where it is reflected off the first couple of metal layers. This image is collected by the microscope objective and viewed on the second black box beam splitter with the CCD camera. This allows us to visualize exactly where the laser is hitting.

A second microscope objective is located above the device and is attached to a CCD camera sensitive to visual wavelengths. Both objectives are aligned, which allows us to see both images at once. This is useful for locating landmarks on the top image which may not be easily visible from the back side.

The DUT is mounted on a movable platen which moves relative to the two microscope objectives. A computer-controlled motion stage is able to position the DUT with 100-nm precision. Custom computer programs are able to perform different automated scanning functions and synchronize the data collection process with the device position. These are shown in Figure 4. An optical breadboard is provided for fastening the test article to the platen.

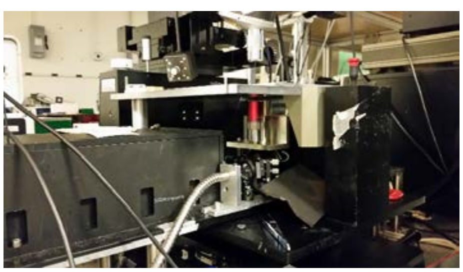

Figure 4 - Photograph of the microscope and positioning stages.

Data is typically collected through a high-speed oscilloscope. Our primary oscilloscope is a LeCroy LabMaster 36zi, capable of measuring 8 simultaneous channels with a 36 GHz bandwidth at 80 Gsamples/s. We record the transient behaviors of the DUT as well as the photodiode for every laser pulse.

LATCHUP TESTING

In a latchup test, one usually monitors the current through the device as it is irradiated with heavy ions or laser pulses. Upon detection of an over-current event, the power supply voltage is removed and this quenches the sustaining latchup current. This must take place quickly to prevent damaging the device. Monitoring the power supply current through a remote programming interface such as GPIB, USB or Ethernet may take 10's of milliseconds to detect a latchup event and send commands to turn the supply off. Since our laser repetition rate is 1 kHz, we need to be able to detect a latchup event, remove the current path, and restore power in under 1 ms.

Commented [P1]: I do not understand this sentence. Maybe there is some errors.

Latchup Detect and Reset Circuit

We have designed a circuit for monitoring the current through a device, detecting a latchup event, and automatically removing the latchup current path. The schematic is shown in Figure 5. The circuit uses a high common-mode fixed-gain amplifier to measure the voltage across a current-sense resistor. The amplifier output is compared with a reference voltage set with a potentiometer. When the device current exceeds the reference, the output of the comparator will go low. The microcontroller will detect this change and turn off the solid-state relay that is used to complete the current path. The relay will be re-engaged after a programmable delay. The relay is kept off long enough to ensure the latchup event is quenched. It is turned on early enough to give the circuit time to stabilize before the next laser pulse. A photograph of the prototype circuit is shown in Figure 6. Figure 7 shows schematically how the test device is connected to the detection circuit. The detection circuit is connected in series with the DUT while the outputs are monitored on the oscilloscope.

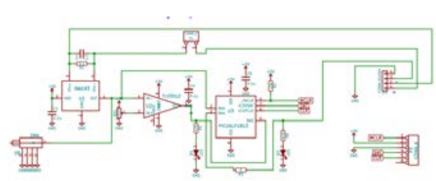

Figure 5 - Schematic of the latchup detecting and reset circuit.

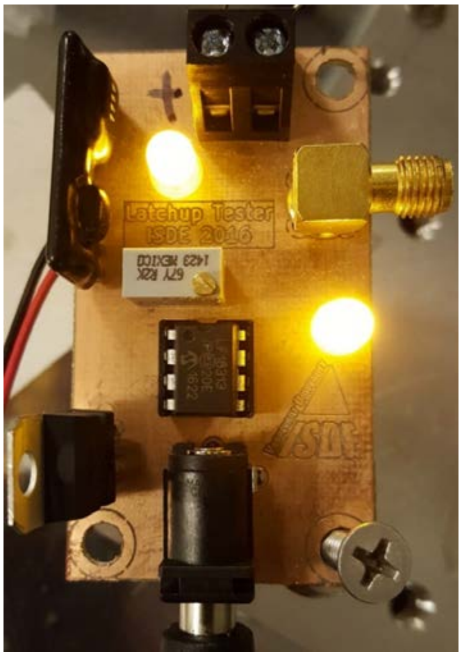

Figure 6 - Photograph of the latchup detection and correction circuit.

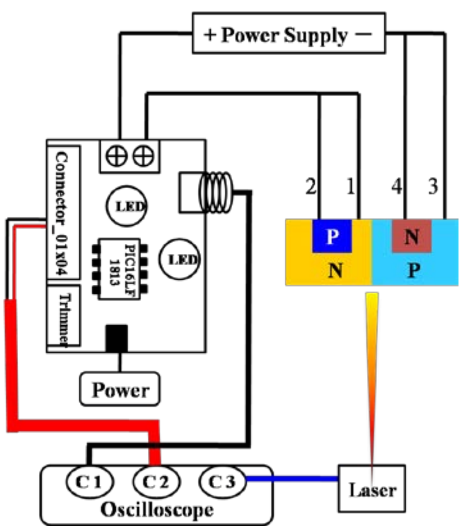

Figure 7 - Shows the connections between the DUT, oscilloscope, and latchup detection and reset circuit.

TPA Test Structures

In this paper we demonstrate the use of a TPA laser to simulate latchup on a set of test structures fabricated in the Jazz Semiconductor 180-nm process. The test structures were designed to imitate the layout of the well structures of a typical SRAM cell. Figure 8 shows the layout details and cross section. Separate off-chip contacts are provided for the n-well, p-well, n+, and p+ diffusions.

The devices here are provided in die form. We have bonded them to a package with a hole in the middle to permit the laser to reach the back side of the die. Parts that are encapsulated in plastic packages can easily be etched to expose the die. These may be soldered to a PCB with a hole drilled in it or mounted in a modified IC socket.

The device is biased as a diode during the latchup tests, with the p+ and n-well regions tied to VDD and the n+ and p-well regions grounded. A typical VDD for this process is 3.3V.

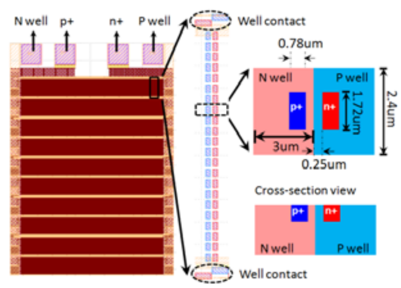

Figure 8 - Test structure layout and cross section. The design is designed to imitate the well structures in a typical SRAM cell.

RESULTS

Figure 9 shows the data recorded in a typical latchup event. We record the energy on the photodiode (blue), the voltage from the current monitoring amplifier (black), and the on-off signal from the microcontroller to the relay (red). Figure 9 shows 6 laser pulses that cause latchup and one that does not. Note that there is one millisecond between each event. This shows that we are operating at the repetition rate of the laser, and are able to detect and reset events at a rate to allow each laser pulse the opportunity to cause a latchup. It can be seen on the expanded view in Figure 9 that after the laser pulse there is a delay before the latchup current starts to rise. The delay and rise-time of the latchup current is mostly a function of the time and slew response of the amplifier. The actual latchup current will rise much faster. After a short time, the microcontroller removes power to relay.

We use the energy modulator to strike the device with a range of energies as a way to determine the onset energy for latchup. Figure 10 shows a typical scope capture. For lower laser energies (blue) the reset line (red) stays high, since no latchup occurs. At higher energies, the latchup events cause the reset line to go low. Due to slight variations with each pulse, there is a probability that a pulse near the threshold may or may not cause a latchup. We perform a statistical analysis on the results and use the 50% probability point to define the energy threshold. An example of this is shown in Figure 11.

These measurements are repeated over the area of interest on the part. The control software coordinates the positioning and data-collection processes. Automated software routines are able to analyze the data for all energies at each position. By analyzing the threshold energy at each location, we are able to create a sensitivity map of the device. An example is shown in Figure 12. As one would expect, the energy required to cause a latchup increases significantly near the well contacts where the contact resistance to the parasitic transistors is lowest.

The sensitive area can be estimated by summing the area where the SEL latchup is below a specified threshold. The SEL-sensitive area is a useful metric for comparing similar devices, as the SEL rate will be proportional to this value. The actual SEL rate cannot be fully computed since there is not a straightforward mapping between laser energy and heavy-ion LET.

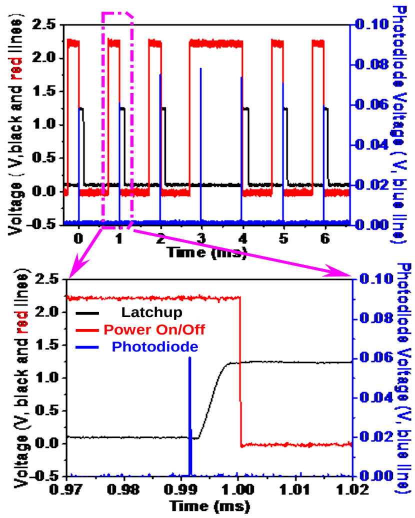

Figure 9 - Oscilloscope captures for a series of laser pulses that do and do not cause latchup.

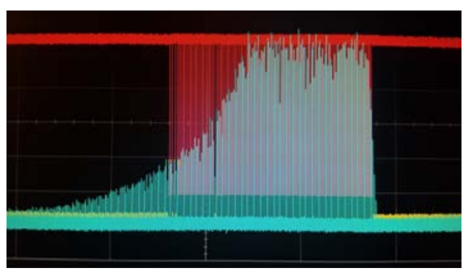

Figure 10 - 400 laser pulses with a modulated energy. The laser pulse energies are shown in blue. The reset signal is shown in red. The reset pulse is only triggered for higher energy events.

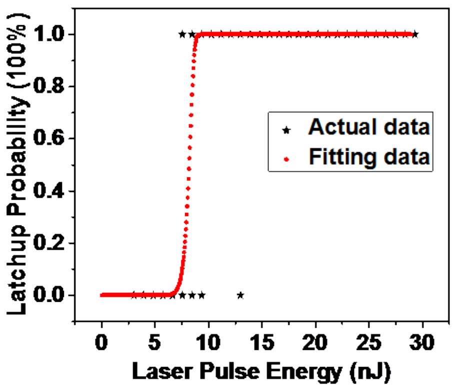

Figure 11 - Statistical analysis of the pulse variation to determine the threshold.

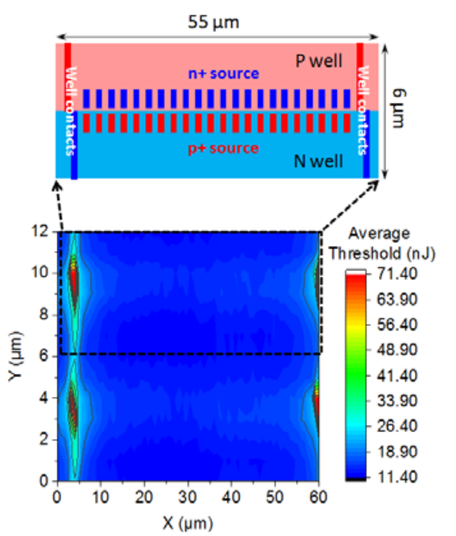

Figure 12 - Heat map showing the sensitivity of a row of test structures.

CONCLUSIONS

In this paper, we have demonstrated how a pulsed laser technique can be used to map the SEL sensitivity of a device. Although it has been shown here on a simple test circuit for clarity, it is applicable to devices of any complexity.

With this technique, it is possible to determine if a device may be sensitive to SEL, estimate the worst-case cross section, and compare the relative sensitivities of different devices without heavy-ion irradiation.

This methodology is easily adapted to other radiation-induced single-event phenomena such as single-event functional interrupt (SEFI), single-event transients (SETs), or single-event upsets (SEUs).

References

1. https://radcentral.jpl.nasa.gov/
2. https://radhome.gsfc.nasa.gov/
3. https://escies.org/labreport/radiationList
4. K. Ni; A. L. Sternberg; E. X. Zhang; J. A. Kozub; R. Jiang; R. D. Schrimpf; R. A. Reed; D. M. Fleetwood; M. L. Alles; D. McMorrow; J. Lin; A. Vardi; J. del Alamo, "Understanding Charge Collection Mechanisms in InGaAs FinFETs Using High-Speed Pulsed-Laser Transient Testing with Tunable Wavelength," in *IEEE Transactions on Nuclear Science* , vol.PP, no.99, pp.1-1
5. W. G. Bennett *et al*., "Single- and Multiple-Event Induced Upsets in HfO2/ Hf 1T1R RRAM," in *IEEE Transactions on Nuclear Science*, vol. 61, no. 4, pp. 1717-1725, Aug. 2014.
6. Y. P. Chen *et al*., "Single-Event Transient Induced Harmonic Errors in Digitally Controlled Ring Oscillators," in *IEEE Transactions on Nuclear Science*, vol. 61, no. 6, pp. 3163-3170, Dec. 2014.
7. W. G. Bennett *et al*., "Experimental Characterization of Radiation-Induced Charge Sharing," in *IEEE Transactions on Nuclear Science*, vol. 60, no. 6, pp. 4159-4165, Dec. 2013.
8. D. H. Habing, "The Use of Lasers to Simulate Radiation-Induced Transients in Semiconductor Devices and Circuits," in IEEE Transactions on Nuclear Science, vol. 12, no. 5, pp. 91-100, Oct. 1965.
9. D. McMorrow, W. T. Lotshaw, J. S. Melinger, S. Buchner and R. L. Pease, "Subbandgap laser-induced single event effects: carrier generation via two-photon absorption," in *IEEE Transactions on Nuclear Science*, vol. 49, no. 6, pp. 3002-3008, Dec 2002.

Commented [RDS2]: Where is this discussed?

Commented [P3]: Ref 8 is missed.